

Theory of Kondo Effect in Superconductors II.

— Specific Heat Jump at the Transition Temperature —

Shin'ichi ICHINOSE

Department of Physics, Nagoya University, Nagoya, Japan

Thermodynamic properties of superconducting alloys near the transition temperature are studied within the interpolation approximation which is constructed so as to coincide with theories in limiting cases. Using this approximation, the specific heat jump at the transition temperature is calculated in the case of the magnitude of the impurity spin being $1/2$. The result shows a continuous change of the specific heat jump with T_K/T_{co} from the Abrikosov-Gorkov value to essentially BCS-like behavior in contrast to the Müller-Hartmann-Zittartz theory. One has an example of a cross over between a weak coupling situation at $T_K/T_{co} \ll 1$ and a strong coupling behavior at $T_K/T_{co} \gg 1$. The Hartree-Fock theory is also discussed in connection with the present calculation.

§1. Introduction

In the first paper of this series,¹⁾ where the effect of magnetic impurities on superconductivity was investigated, we presented the interpolation approximation which covers two limiting cases; $T(\text{and/or } \epsilon) \gg T_K$ and $T(\text{and } \epsilon) \ll T_K$ in the same framework. We showed that contrary to the Müller-Hartmann-Zittartz theory (MZ),²⁾ a finite critical concentration is always obtained for any value of the Kondo temperature and also that the upper critical field at zero temperature depends on the magnetic impurity concentration in contrast to Maki's theory.³⁾ It is left as a next problem to make clear the thermodynamic and magnetic properties near the transition point. In this paper, which may be regarded as an extension of the first paper, we calculate the specific heat jump at the transition temperature ΔC and discuss the relation between our calculation and other theories: in particular, the Hartree-Fock theory⁴⁾ and the MZ theory.²⁾ Here, discussion is mainly concentrated on the properties of the four-particle Green's function which relates to the thermodynamic properties near T_c (the superconducting transition temperature) as well as on the behavior of the specific heat jump ΔC itself.

As one knows from the Abrikosov-Gorkov theory (AG)⁵⁾ that the specific heat jump of a superconductor is strongly influenced by the presence of magnetic impurities. It seems to be generally true that the reduction of the specific heat jump corresponds to the pair-breaking situations. On the other hand if the BCS description is relevant, the jump is proportional to T_c , and thus the reduction in the jump proportional to the T_c reduction.

Looking back in perspective at a successive wave of theories of the Kondo effect, we see that a very simple picture emerges.

When temperature and/or energy goes through T_K which separates two physically different regimes, the qualitative physics of the system changes. Though the intermediate range is very complicated, two limits $T(\text{and/or } \epsilon) \gg T_K$ and $T(\text{and } \epsilon) \ll T_K$ are both conceptually very simple, albeit different. At $T \gg T_K$ and/or $\epsilon \gg T_K$, the impurity spin is essentially free to fluctuate, driven by the thermal agitation. As it provides a real degree of freedom, as shown in the Curie susceptibility in the normal state, the strongly temperature dependent pair-breaking mechanism acts upon the system in the superconducting state and leads to the strong reduction of the specific heat jump. On the other hand, at $T \ll T_K$ and $\epsilon \ll T_K$, the impurity spin is locked into a singlet bound state and no longer takes part in dynamics. However, the virtual excitation of the impurity at this state is possible as far as T_K/T and T_K/ϵ are finite.⁶⁾ It follows that in a superconductor one electron of mates of the Cooper pair polarizes the impurity at the singlet bound state and that polarization is felt by another electron. This mechanism gives an effective repulsion between two electrons. Near $T_K/T_{co} = \infty$, the reduction in the specific heat jump is proportional to the T_c reduction. Therefore we can expect that the BCS-like behavior which is typical for non-pair-breaking situations should show up in the specific heat jump.

In the cross over region $T \sim T_K$ and/or $\epsilon \sim T_K$, the situation is very complicated and we cannot draw a simple physical picture of the magnetic impurities. If one insists on mathematical rigor, there is only one line of attack to describe the cross over: numerical intergration, as done by Wilson.⁷⁾ However, if our purpose is mainly to describe the gradual change of the impurity electronic state from the magnetic behavior to the nonmagnetic ones, we can get

around this difficulty by introducing the interpolation approximation. The strong reduction of the specific heat jump in this region can be easily observable.

These behaviors are best visualized in the quantity C^* which is introduced as the initial slope of the specific heat jump at T_c . As C^* depends exclusively on single-impurity parameters, it may be used to determine the Kondo temperature. The quantity C^* is equal to 1 for a BCS-superconductor; i.e. when the transition temperature is depressed by the effective repulsive interaction mechanism. However, C^* is larger than 1 for a pair-breaking situation, in particular the largest value of C^* must be observed for a superconductor containing magnetic impurities of which the Kondo temperature is of the same order as T_{c0} . Such behaviors are qualitatively in good agreement with experiments.¹¹⁾ Quite generally we can say that the size of the quantity C^* reveals the magnetic character of the single impurity imbedded in a superconductor. From these consideration, we expect that C^* approaches the BCS-value, $C^*=1$ in the limit of high Kondo temperature, $T_K/T_{c0} \rightarrow \infty$ and then the magnetic impurity loses its magnetic character, contrary to the MZ theory.

This paper is arranged as follows: Section 2 is devoted to the general formulation of the self-consistent equation for Δ up to the third order, taking account of dynamical properties of impurities. In §3, we discuss the four-particle Green's function for the two limiting cases and construct an interpolation expression for them. Using it, we calculate the specific heat jump at the transition temperature in §4. In §5, we give summary and comments on some other works.

§2. Formulation

As in Ref.1), hereafter referred to as I, we study the self-consistent equation for the order parameter Δ , taking account of the dynamical behavior of impurities. Following AG, the self-consistent equation is given up to the third order in Δ by

$$\Delta = |g|Q(T)\Delta + |g|B(T)\Delta^3 \quad (2.1)$$

$$Q(T) = \int_0^{1/T} d\tau' \int d^3r' \langle T_\tau \{ \tilde{\Psi}_\uparrow(r, \tau) \tilde{\Psi}_\downarrow(r, \tau) \tilde{\Psi}_\downarrow^+(r', \tau') \tilde{\Psi}_\uparrow^+(r', \tau') \} \rangle \quad (2.2)$$

$$B(T) = \int_0^{1/T} \cdots \int_0^{1/T} d\tau_1 \cdots d\tau_3 \int \cdots \int d^3r_1 \cdots d^3r_3 \langle T_\tau \{ \tilde{\Psi}_\uparrow(r, \tau) \tilde{\Psi}_\downarrow(r, \tau) \times \tilde{\Psi}_\downarrow^+(r_1, \tau_1) \tilde{\Psi}_\uparrow^+(r_1, \tau_1) \tilde{\Psi}_\uparrow^+(r_2, \tau_2) \tilde{\Psi}_\downarrow(r_2, \tau_2) \tilde{\Psi}_\downarrow^+(r_3, \tau_3) \tilde{\Psi}_\uparrow^+(r_3, \tau_3) \} \rangle, \quad (2.3)$$

where $\tilde{\Psi}_\sigma^+$ and $\tilde{\Psi}_\sigma$ are respectively the Heisenberg representation of the creation and annihilation operators of conduction electrons with spin σ and $\langle \cdots \rangle$ denotes both the statistical average and the average over the impurity distribution.

[1] We must first calculate the two-particle Green's function $Q(T)$. This is done in I, where it is found that

$$Q(T) = T \sum_{\omega} \sum_{\mathbf{k}} \gamma(\omega) G_{\mathbf{k}}(\omega) G_{-\mathbf{k}}(-\omega) \quad (2.4)$$

$$G_{\mathbf{k}}(\omega) = \frac{1}{i\omega - \xi_{\mathbf{k}} - \Sigma(\omega)}, \quad (2.5)$$

where $G_{\mathbf{k}}(\omega)$ is the renormalized one-particle Green's function. Here, $\omega = (2n+1)\pi T$, $\xi_{\mathbf{k}}$ is the one-electron energy of conduction electrons, and $\Sigma(\omega)$ is the self-energy correction due to impurities.

In the case of the electron-hole symmetry, the vertex correction $\gamma(\omega)$ which appears in Eq.(2.4) is given by

$$\gamma(\omega) = \frac{|\omega| + |\sum(\omega)|}{|\omega| + n\alpha(\omega)} \cdot \frac{1 + \frac{n}{4T_K \rho} [\phi_2 - \phi_1 f(\omega)]}{1 + \frac{n}{4T_K \rho} \phi_2}, \quad (2.6)$$

where ρ is the density of states of conduction electrons per atom per spin, n is the impurity concentration and $\alpha(\omega)$ is the pair-breaking parameter which is given by Eq.(3.19) in I and ϕ_k is written by

$$\phi_k(T, n) = \pi T \int_{\omega} \frac{\{f(\omega)\}^k}{|\omega| + n\alpha(\omega)}, \quad (2.7)$$

with $f(\omega) = (1 + \frac{\pi|\omega|}{4T_K})^{-2}$. For the later convenience, we rewrite the vertex correction $\gamma(\omega)$ by the use of two renormalization factors; $\eta_1(\omega)$ and $\eta_2(\omega)$,

$$\gamma(\omega) = \frac{\eta_1(\omega)}{\eta_2(\omega)} \quad (2.8)$$

$$|\omega| \eta_1(\omega) = |\omega| + |\sum(\omega)| \quad (2.9)$$

$$|\omega| \eta_2(\omega) = [|\omega| + n\alpha(\omega)] \cdot \frac{1 + \frac{n}{4T_K \rho} \phi_2}{1 + \frac{n}{4T_K \rho} [\phi_2 - \phi_1 f(\omega)]}, \quad (2.10)$$

where N is the number of atoms.

[2] Next we consider the four-particle Green's function $B(T)$.

Since we will describe the whole aspect of the expressions of $B(T)$

including two limiting cases in the following section, here we give only the formal expression of $B(T)$. This is done by introducing the third renormalization factor $\eta_3(\omega)$ as follows;

$$B(T) = - \frac{\pi N \rho}{2} T \sum_{\omega} \frac{|\omega| \eta_3(\omega)}{[|\omega| \eta_2(\omega)]^4} \quad (2.11)$$

For the later convenience, we separate $\eta_3(\omega)$ into the n-independent part and the n-linear part.

$$|\omega| \eta_3(\omega) = |\omega| + \frac{n}{2\pi\rho} \chi(\omega) \quad (2.12)$$

If we neglect the second term in Eq.(2.12), the contributions from the higher order processes of the impurity scattering beyond the AG type theory drop off in the four-particle Green's function $B(T)$, as will be shown later.

§3. Approximation for Vertex and Four-particle Green's function

In this section we examine the behavior of the vertex $\gamma(\omega)$ and the four-particle Green's function $B(T)$ for two limiting cases, and propose the approximate expression for $B(T)$ which is expected to be valid in the wide range of T in the s-d limit of impurities. The Hartree-Fock theory and the MZ theory are also discussed in connection with the present calculation.

[1] When $T \gg T_K$ and/or $\epsilon \gg T_K$, the Kondo effect can be taken into account by replacing J (the s-d exchange interaction) by the spin-flip part of the t-matrix. It is given in the MZ theory by

$$\tau(\omega) = -\frac{1}{2N\rho} \left[\left(\ln \frac{|\omega|}{T_K} \right)^2 + \pi^2 S(S+1) \right]^{-\frac{1}{2}} \quad (3.1)$$

If we employ the most divergent approximation,¹²⁾ the spin-non flip part $t(\omega)$ of the t -matrix in a normal metal is equal to zero. This fact leads us to conclude that the vertex corrections, which are related to the spin-non flip part $t(\omega)$, drop off in the four-particle Green's function $B(T)$. So we need to calculate $B(T)$ in the approximation beyond the most divergent one even in the magnetic region. In order to demonstrate what type of contributions are included in the present calculation, we show in Fig.1

Fig. 1

the Feynman diagrams of all the contributions to $B(T)$.

As Shiba pointed out in Ref.4), there exists a certain relation between the Hartree-Fock theory including the classical spin theory and the MZ theory. It is shown that the four-particle Green's function for the Kondo spin within a certain approximation can be derived from the calculations for the classical spin by the replacement $|\tau(\omega)|_c$ by $|\tau(\omega)|$, of Eq. (3.1), and S^4 by $S(S+1)[S(S+1) - \frac{1}{3}]$ where

$$\tau(\omega)_c = -\frac{J}{2N} \cdot \frac{1}{1 + \left(\frac{1}{2}JS\pi\rho\right)^2} \quad (3.2)$$

Let us now ask for the four-particle Green's function on this principle. The four-particle Green's function for the classical spin becomes (see Appendix A)

$$B(T) = - \frac{\pi N \rho}{2} T \sum_{\omega} \frac{|\omega| + \frac{16n}{\pi \rho} [\pi N \rho S |\tau(\omega)|_c]^4}{[|\omega| + \frac{1}{\tau_s}]^4} \quad (3.3)$$

Thus in the case of the Kondo spin, we arrive at

$$B(T) = - \frac{\pi N \rho}{2} T \sum_{\omega} \frac{|\omega| + \frac{n}{2\pi \rho} \chi(\omega)}{[|\omega| \eta_2(\omega)]^4} \quad (3.4)$$

$$\chi(\omega) = 2S(S+1) [S(S+1) - \frac{1}{3}] (\tilde{J}\pi\rho)^4 \quad (3.5)$$

where

$$\tilde{J} = - \frac{1}{\rho} [(\ln \frac{|\omega|}{T_K})^2 + \pi^2 S(S+1)]^{-1/2} \quad (3.6)$$

Although the analogous expression was derived in the MZ theory, we notice that the spin term is given by $S(S+1)[S(S+1) - \frac{1}{3}]$ instead of $[S(S+1)]^2$ for reasons of the non-commutative nature of the spin in contrast to their result.

[2] On the other hand, when $T \ll T_K$ and $\epsilon \ll T_K$, we study the behavior of the magnetic impurities based on the Yamada-Yosida theory of the Anderson model.⁹⁾ Using the results of the Yamada-Yosida theory, we find for the renormalization factor $\eta_1(\omega)$

$$|\omega| \eta_1(\omega) \simeq |\omega| + \frac{n}{\pi \rho} \cdot \frac{1}{1+|\bar{\omega}|} \quad (3.7)$$

with $|\bar{\omega}| = \frac{\pi |\omega|}{4T_K}$, ~~while we find~~ ^{and} for the renormalization factor $\eta_2(\omega)$

$$|\omega| \eta_2(\omega) \simeq \frac{|\omega| + \frac{n}{\pi \rho} \cdot \frac{|\bar{\omega}|}{(1+|\bar{\omega}|)^2}}{1 - \frac{n}{\pi \rho} \cdot \frac{\bar{\phi}_1}{(1+|\bar{\omega}|)^2}} \quad (3.8)$$

with

$$\bar{\phi}_1 = \phi_1 / T_K = \frac{\pi}{4T_K} \cdot \frac{\phi_1}{1 + \frac{n}{4T_K \rho} \phi_2} \quad (3.9)$$

Notice that ϕ_1 corresponds to the quantity $\phi = -\Delta_d / \Delta_0$ in the Hartree-Fock theory,⁴⁾ and $T_c \bar{\phi}_1$ is always smaller than unity (e.g. in the case of the low impurity concentration $T_{co} \bar{\phi}_1 = 10^{-3} \sim 10^{-2}$ for reasonable values of T_K / T_{co}).*) Using Eqs.(3.7) and (3.8), we have

$$\gamma(\omega) = \frac{|\omega| + \frac{n}{\pi\rho} \cdot \frac{1}{1+|\bar{\omega}|}}{|\omega| + \frac{n}{\pi\rho} \cdot \frac{|\bar{\omega}|}{(1+|\bar{\omega}|)^2}} \left[1 - \frac{n}{\pi\rho} \cdot \frac{\bar{\phi}_1}{(1+|\bar{\omega}|)^2} \right] \quad (3.10)$$

Now we turn to the study of the properties of the four-particle Green's function $B(T)$. Typical diagrams of $B(T)$ look like Fig.2.

Fig. 2

The contributions to $B(T)$ can be classified in general into the Hartree-Fock type contribution (Fig.2a) and the non-H.F. type ones (Fig.2b). The former contributions can be derived from the Hartree-Fock results by the replacement of the d-electron Green's function $G_d(\omega) = [i\omega + i\Gamma \text{sgn } \omega]^{-1}$ by

$$G_d(\omega) = -\frac{i}{\Gamma} \cdot \frac{\text{sgn } \omega}{1 + \frac{\pi|\omega|}{4T_K}} \quad (3.11)$$

and the effective interaction between d-electrons $\Gamma_d = \tilde{U} = U / (1 + \frac{U}{\pi\Gamma})$ by

$$\Gamma_d = \frac{\pi^2 \Gamma^2}{4T_K} \quad (3.12)$$

*) $T_c \bar{\phi}_1 \sim \frac{T_c}{T_K} \cdot \frac{\ln \frac{T_K}{T_c}}{1 + \frac{n}{4T_K \rho} \ln \frac{T_K}{T_c}}$ for $T_c < T_K$.

On the other hand, the latter corresponds to the contributions of diagrams which are never considered in the H.F. approximation. Although $\chi(\omega)$ at $|\omega|/T_K < 1$ is a very complicated function of $|\omega|/T_K$, fortunately we can pick out the leading term; the $|\omega|$ -linear contribution of $\chi(\omega)$, as far as the condition $T \ll T_K$ is satisfied. This calculations can be done by standard methods, but requires complicated analysis. From these analysis we see that some of the H.F. type contributions give us the leading term of $\chi(\omega)$. The leading term of $\chi(\omega)$ becomes (see Appendix B)*)

$$\chi(\omega) = \frac{\pi|\omega|}{2T_K} \quad (3.13)$$

[3] Now we turn to the intermediate region. In this region, we should take interpolation of Eq.(3.5) and (3.13). Though interpolation is rather arbitrary, we must determine it so that $\chi(\omega)$ becomes a smooth, continuous function at $|\omega| = \frac{4T_K}{\pi}$. We choose the following expression for convenience:

$$\chi(\omega) = \begin{cases} \frac{\pi|\omega|}{2T_K} - \frac{2}{3} \left(\frac{\pi|\omega|}{4T_K} \right)^2 - \frac{2}{9} \left(\frac{\pi|\omega|}{4T_K} \right)^3 & \frac{\pi|\omega|}{4T_K} < 1 \\ \frac{10}{9} \left[\frac{\frac{3}{4}\pi^2}{(\ln \frac{\pi|\omega|}{4T_K})^2 + \frac{3}{4}\pi^2} \right]^2 & \frac{\pi|\omega|}{4T_K} > 1 \end{cases} \quad (3.14)$$

where the magnitude of the impurity spin is assumed 1/2. Notice that in the first expression of Eq.(3.14) only the coefficient of the linear term in $|\omega|$ is meaningful, because the coefficients of the quadratic and cubic terms are not exact. The

*) This expression consists with the result previously obtained by Matsuura by a different method.¹⁴⁾ One may regard therefore our calculation as a sort of a justification of his result, as far as the main contribution is concerned.

numerical calculation of $\chi(\omega)$ is shown in Fig.3. It takes the

Fig. 3

maximum value $\frac{10}{9}$ at $\frac{\pi|\omega|}{4T_K} = 1$. The expression for the high frequency region is similar to the expression of $\chi(\omega)$ in the MZ theory, except for the numerical factor. There remains some ambiguity in the form of $\chi(\omega)$ in the region $\omega \sim T_K$.

§4. Specific heat jump at the transition temperature

We first calculate the thermodynamic potential to derive the thermodynamic quantity near the transition temperature. The difference of the thermodynamic potential between the superconducting and normal states is expressed as⁴⁾

$$\Omega_s - \Omega_n = \int_0^{\Delta} d\Delta' (\Delta')^2 \frac{d(1/|g|)}{d\Delta'} \quad , \quad (4.1)$$

which reduces to

$$\Omega_s - \Omega_n = \frac{1}{2} B(T) \Delta^4 \quad , \quad (4.2)$$

near T_c . Here use has been made of the relation

$$\delta\left(\frac{1}{|g|}\right) = 2B(T) \Delta \delta\Delta \quad , \quad (4.3)$$

which is derivable from Eq.(2.1) for $T \lesssim T_c$. As evident from Eq.(2.1), Δ^2 is proportional to $1-T/T_c$ near T_c in the form

$$\Delta^2 = -\frac{N\rho}{B(T_c)} \cdot \left(1 + T_c \frac{\partial B_o(T)}{\partial T} \Big|_{T=T_c}\right) \left(1 - \frac{T}{T_c}\right), \quad (4.4)$$

where $B_o(T)$ is expressed as

$$\begin{aligned} B_o(T) &= \frac{1}{|g|N\rho} - \ln \frac{T}{T_{co}} - \frac{Q(T)}{N\rho} \\ &= -\phi(T) + \frac{n}{4T_K\rho} \cdot \frac{[\phi_1(T)]^2}{1 + \frac{n}{4T_K\rho} \phi_2(T)}, \end{aligned} \quad (4.5)$$

where $\phi(T)$ is the quantity introduced in I:

$$\phi(T) = \pi T \int_{\omega} \left[\frac{1}{|\omega| + n\alpha(\omega)} - \frac{1}{|\omega|} \right] \quad (4.6)$$

Using Eqs. (4.2) and (4.4), we find for ΔC

$$\begin{aligned} \Delta C &= -T_c \frac{\partial^2 (\Omega_s - \Omega_n)}{\partial T^2} \Big|_{T=T_c} \\ &= -\frac{T_c (N\rho)^2}{B(T_c)} \cdot \left(\frac{1}{T_c} + \frac{\partial B_o(T)}{\partial T} \Big|_{T=T_c} \right)^2, \end{aligned} \quad (4.7)$$

which finally gives

$$\frac{\Delta C}{\Delta C_o} = -\frac{7\zeta(3)}{8\pi^2} \cdot \frac{N\rho}{B(T_c)} \cdot \frac{T_c}{T_{co}} \left(\frac{1}{T_c} + \frac{\partial B_o(T)}{\partial T} \Big|_{T=T_c} \right)^2, \quad (4.8)$$

where $\Delta C_o = \frac{8\pi^2 N\rho T_{co}}{7\zeta(3)}$ is the specific heat jump of the pure superconductor.

The reduction of the specific heat jump at T_c is most easily observed by evaluating

$$c^* = \frac{d(\Delta C/\Delta C_o)}{d(T_c/T_{co})} \Big|_{T_c=T_{co}} \quad (4.9)$$

Since it is tedious to write down long expression for $\Delta C/\Delta C_o$

and C^* , we show the expressions for them only for two limiting cases and point out some of the features.

[1] When $T \gg T_K$, ϕ_1 and ϕ_2 can be neglected. If we replace $\alpha(\omega)$ by $\alpha(T)$, then Eq.(4.5) can be approximated by

$$B_o(T) \approx -\ln \frac{T_c}{T_{co}} + \frac{n\alpha(T_c)}{2\pi} \psi^{(1)} \left(\frac{1}{2} + \frac{n\alpha(T_c)}{2\pi T_c} \right) \left(\frac{1}{T} - \frac{1}{T_c} \right), \quad (4.10)$$

near T_c . Here $\alpha(T_c)$ is defined by

$$\alpha(T_c) \approx \frac{1}{2\pi\rho} \cdot \frac{\frac{3}{4}\pi^2}{\left(\ln \frac{T_c}{T_K}\right)^2 + \frac{3}{4}\pi^2}. \quad (4.11)$$

When we also replace $\chi(\omega)$ by $\chi(T)$, $B(T_c)$ is expressed as

$$B(T_c) \approx \frac{N\rho}{16(\pi T_c)^2} \left[\psi^{(2)} \left(\frac{1}{2} + \alpha_c \right) + \frac{1}{3} \alpha_c (1-\delta) \psi^{(3)} \left(\frac{1}{2} + \alpha_c \right) \right], \quad (4.12)$$

where $\delta = \frac{20}{9} \pi \rho \alpha(T_c)$, which reduces to zero in the AG limit, and $\alpha_c = \frac{n\alpha(T_c)}{2\pi T_c}$. Using Eqs.(4.11) and (4.12) in Eq.(4.8), we find for $\Delta C/\Delta C_o$

$$\frac{\Delta C}{\Delta C_o} \approx \frac{T_c}{T_{co}} \cdot \frac{\psi^{(2)} \left(\frac{1}{2} \right) \left[1 - \alpha_c \psi^{(1)} \left(\frac{1}{2} + \alpha_c \right) \right]^2}{\psi^{(2)} \left(\frac{1}{2} + \alpha_c \right) + \frac{1}{3} \alpha_c (1-\delta) \psi^{(3)} \left(\frac{1}{2} + \alpha_c \right)}, \quad (4.13)$$

where $\psi^{(n)}(z)$ is the poly-gamma function. One easily finds that Eq.(4.13) corresponds to the result of the MZ theory,²⁾ except for the numerical factor of δ .

Calculations of C^* can be simplified using the approximations

plified using the approximations

$$\alpha(T_{CO}) \approx \frac{3\pi}{8\rho} \left(\ln \frac{T_K}{T_{CO}}\right)^{-2} \quad (4.14)$$

$$-\left. \frac{dn}{dt_c} \right|_{t_c=1} \approx \frac{32\rho T_{CO}}{3\pi^2} \left(\ln \frac{T_K}{T_{CO}}\right)^2 \quad (4.15)$$

$$\delta \approx \frac{\pi^2}{6} \left(\ln \frac{T_K}{T_{CO}}\right)^{-2} \quad (4.16)$$

where $t_c \equiv T_c/T_{CO}$. The result is given by

$$C^* = C_{AG}^* + \frac{\pi^4}{126 \zeta(3)} \left(\ln \frac{T_K}{T_{CO}}\right)^{-2} \quad (4.17)$$

where

$$C_{AG}^* = 3 - \frac{4\pi^2}{21 \zeta(3)} = 1.436$$

One easily finds that C^* approaches the AG value C_{AG}^* in the limit $T_{CO}/T_K \rightarrow \infty$.

[2] On the other hand, if $T_K \gg T$, we can put

$$\phi_0(T_c) \approx \phi_1(T_c) \approx \phi_2(T_c) \approx \frac{1}{|\tilde{g}|N\rho} \quad (4.18)$$

where

$$|\tilde{g}| = |g| - \frac{n}{4NT_K\rho^2} \quad (4.19)$$

Using the approximations

$$|\omega| \eta_3(\omega) \approx \left(1 + \frac{n}{4T_K\rho}\right) |\omega| \quad (4.20)$$

$$|\omega| + n\alpha(\omega) \approx \left(1 + \frac{n}{4T_K\rho}\right) |\omega| \quad (4.21)$$

we can greatly simplify the calculations of $B(T_c)$ and $\left. \frac{\partial B_o(T)}{\partial T} \right|_{T=T_c}$. These results are given by

$$B(T_c) \approx - \frac{7\zeta(3)N\rho}{8(\pi T_c)^2} \cdot \frac{1}{\left(1 + \frac{n}{4T_K\rho}\right)^3} \cdot \frac{1}{\left(1 + \frac{n}{4T_K\rho} \cdot \frac{1}{|\tilde{g}|N\rho}\right)^4} \quad (4.22)$$

$$\left. \frac{1}{T_c} + \frac{\partial B_o(T)}{\partial T} \right|_{T=T_c} \approx \frac{1}{T_c} \cdot \frac{1}{1 + \frac{n}{4T_K\rho}} \cdot \frac{1}{\left(1 + \frac{n}{4T_K\rho} \cdot \frac{1}{|\tilde{g}|N\rho}\right)^2} \quad (4.23)$$

From Eqs. (4.22) and (4.23) we have^{*}

$$\frac{\Delta C}{\Delta C_o} \approx \frac{T_c}{T_{co}} \left(1 + \frac{n}{4T_K\rho}\right) \quad (4.24)$$

The T_K/T_{co} - dependence of C^* is given by

$$C^* = C_{BCS}^* - \left(\ln \frac{T_K}{T_{co}}\right)^{-2} \quad (4.25)$$

where $C_{BCS}^* = 1$. Here use has been made of the approximation

$$-\left. \frac{dn}{dt_c} \right|_{t_c=1} \approx 4T_K\rho \left(\ln \frac{T_K}{T_{co}}\right)^{-2} \quad (4.26)$$

One easily finds that C^* approaches the BCS-value $C_{BCS}^* = 1$ in the limit of high Kondo temperature, $T_K/T_{co} \rightarrow \infty$, in contrast to the MZ theory.

The behavior of $\Delta C/\Delta C_o$ as a function of T_c/T_{co} is given by the numerical calculation for the wide region of T_K/T_{co} . Results are given in Fig. 4. Here the parameter used for the

Fig. 4

^{*}) If we replace $\frac{1}{4T_K}$ by the state density of the d-electron β_d , we can immediately obtain the result for the nonmagnetic Anderson model. 10)

numerical calculation is $\frac{\omega_D}{\pi T_{co}} = 1169$. In order to calculate Eq. (4.9) in the whole region of T_K/T_{co} , we should carry out the numerical calculation. Results are given in Fig. 5. The initial slope of

Fig. 5.

the specific heat jump becomes maximum where $T_K/T_{co} \approx 1$. The numerical value of T_K/T_{co} at the maximum is not so much meaningful, since it depends on the detail of our interpolation.

§5. Discussion

Throughout this paper we have employed an interpolation approximation to study the thermodynamic properties of superconducting dilute alloys containing magnetic impurities with Kondo effect. Let us give a brief summary of the present calculations and then discuss the relation between the MZ theory and the present one. Our calculations show a continuous change of the specific heat jump with T_K/T_{co} from the AG-value to essentially BCS-like behavior and that the initial slope of the specific heat jump C^* approaches the BCS-value in the limit of high Kondo temperature, $T_K/T_{co} \rightarrow \infty$ in contrast to the MZ theory.

In view of the philosophy of scaling,¹³⁾ we see that the end of an infinite T_K/T_{co} is indeed a fixed point-one in which the physics is completely different from that which prevails near $T_K/T_{co} = 0$. One cannot break the impurity singlet state without an infinite expense of energy: we are left with a nonmagnetic, infinitely repulsive impurity. Therefore the reduction of the

specific heat jump must correspond to the non-pair-breaking situations at the end of an infinite T_K/T_{CO} . From these considerations we can conclude that when T_{CO} goes through T_K , the qualitative physics of the system changes and then one has an example of a cross over between a weak coupling situation at small Kondo temperature $T_K/T_{CO} \ll 1$ and a strong coupling behavior at high Kondo temperature $T_K/T_{CO} \gg 1$.

Acknowledgments

The author would like to express his sincere thanks to Professor Y. Nagaoka and Dr. T. Matsuura for their valuable comments. He is also indebted to Professor H. Shiba for his enlightening discussion, and to Dr. Ichikawa for his aid of numerical calculations.

Appendix A

In this appendix, we compute the four-particle Green's function $B(T)$ for the classical spin,⁸⁾ which is illustrated in Fig.1. The results are given by

$$B_{1-1} = - \frac{\pi N \rho}{2} T \sum_{\omega} \frac{|\omega| + |\sum(\omega)|}{[|\omega| + \frac{1}{\tau_s}]^4} \quad (\text{A.1})$$

$$B_{1-2} = \frac{\pi N \rho}{2} T \sum_{\omega} \frac{\frac{n}{\pi \rho} [\pi N \rho S |\tau(\omega)|_c]^2}{[|\omega| + \frac{1}{\tau_s}]^4} \quad (\text{A.2})$$

$$B_{1-3} = - \frac{\pi N \rho}{2} T \sum_{\omega} \frac{\frac{2n}{\pi \rho} [\pi N \rho S |\tau(\omega)|_c]^4}{[|\omega| + \frac{1}{\tau_s}]^4} \quad (\text{A.3})$$

$$B_{1-4} = - \frac{\pi N \rho}{2} T \sum_{\omega} \frac{\frac{n}{\pi \rho} [\pi N \rho |t(\omega)|_c]^2}{[|\omega| + \frac{1}{\tau_s}]^4} \quad (\text{A.4})$$

$$B_{1-5} = \frac{\pi N \rho}{2} T \sum_{\omega} \frac{\frac{4n}{\pi \rho} [\pi N \rho |t(\omega)|_c]^3}{[|\omega| + \frac{1}{\tau_s}]^4} \quad (\text{A.5})$$

$$B_{1-6} = - \frac{\pi N \rho}{2} T \sum_{\omega} \frac{\frac{2n}{\pi \rho} [\pi N \rho |t(\omega)|_c]^4}{[|\omega| + \frac{1}{\tau_s}]^4} \quad (\text{A.6})$$

$$B_{1-7} = - \frac{\pi N \rho}{2} T \sum_{\omega} \frac{\frac{4n}{\pi \rho} [\pi N \rho S |\tau(\omega)|_c]^2 \pi N \rho |t(\omega)|_c}{[|\omega| + \frac{1}{\tau_s}]^4} \quad (\text{A.7})$$

$$B_{1-8} = - \frac{\pi N \rho}{2} T \sum_{\omega} \frac{\frac{8n}{\pi \rho} [\pi N \rho S |\tau(\omega)|_c]^2 \pi N \rho |t(\omega)|_c}{[|\omega| + \frac{1}{\tau_s}]^4} \quad (\text{A.8})$$

$$B_{1-9} = \frac{\pi N \rho}{2} T \sum_{\omega} \frac{\frac{4n}{\pi \rho} [\pi N \rho S |\tau(\omega)|_c]^2 [\pi N \rho |t(\omega)|_c]^2}{[|\omega| + \frac{1}{\tau_s}]^4} \quad (\text{A.9})$$

$$B_{1-10} = \frac{\pi N \rho}{2} T \sum_{\omega} \frac{\frac{8n}{\pi \rho} [\pi N \rho S | \tau(\omega) |_{\text{c}}]^2 [\pi N \rho | t(\omega) |_{\text{c}}]^2}{[|\omega| + \frac{1}{\tau_s}]^4} \quad (\text{A.10})$$

where τ_s is the relaxation time in the normal state

$$\frac{1}{\tau_s} = \frac{2n}{\pi \rho} [\pi N \rho S | \tau(\omega) |_{\text{c}}]^2 \quad (\text{A.11})$$

Here $t(\omega)_{\text{c}}$ and $\tau(\omega)_{\text{c}}$ are the spin-non flip and spin-flip parts of the t-matrix for the classical spin in a normal metal respectively.

$$t(\omega)_{\text{c}} = \frac{1}{i\pi N \rho} \cdot \frac{(\frac{1}{2} J S \pi \rho)^2 \text{sgn} \omega}{1 + (\frac{1}{2} J S \pi \rho)^2} \quad (\text{A.12})$$

$$| \tau(\omega) |_{\text{c}} = \frac{J}{2N} \cdot \frac{1}{1 + (\frac{1}{2} J S \pi \rho)^2} \quad (\text{A.13})$$

Summing up the contributions from the diagram (1-1) to (1-10) (we denote the total contributions as $B(T)$), we have

$$B(T) = - \frac{\pi N \rho}{2} T \sum_{\omega} \frac{|\omega| + \frac{16n}{\pi \rho} [\pi N \rho S | \tau(\omega) |_{\text{c}}]^4}{[|\omega| + \frac{1}{\tau_s}]^4} \quad (\text{A.14})$$

Here use has been made of the relation

$$\pi N \rho | t(\omega) |_{\text{c}} [1 - \pi N \rho | t(\omega) |_{\text{c}}] = [\pi N \rho S | \tau(\omega) |_{\text{c}}]^2 \quad (\text{A.15})$$

which is derivable from a unitarity relation for the s-matrix.

Appendix B

In this appendix, we estimate the contributions of typical diagrams for $B(T)$ which is illustrated in Fig.2. The results are given by

type (a)

$$B_{a-1} = - \frac{\pi N \rho}{2} T \sum_{\omega} \frac{|\omega| \eta_1(\omega)}{[|\omega| \eta_2(\omega)]^4} \quad (B.1)$$

$$B_{a-2} = - \frac{N_i}{2} T \sum_{\omega} \frac{1}{[|\omega| \eta_2(\omega)]^4} \cdot \frac{1}{(1 + |\bar{\omega}|)^2} \quad (B.2)$$

$$B_{a-3} = 2N_i T \sum_{\omega} \frac{1}{[|\omega| \eta_2(\omega)]^4} \cdot \frac{1}{(1 + |\bar{\omega}|)^3} \quad (B.3)$$

$$B_{a-4} = -N_i T \sum_{\omega} \frac{1}{[|\omega| \eta_2(\omega)]^4} \cdot \frac{1}{(1 + |\bar{\omega}|)^4} \quad (B.4)$$

$$B_{a-5} = 2N_i \bar{\phi}_1^2 T \sum_{\omega} \frac{1}{[|\omega| \eta_2(\omega)]^2} \cdot \frac{1}{(1 + |\bar{\omega}|)^3} \quad (B.5)$$

$$B_{a-6} = 4N_i \bar{\phi}_1^3 T \sum_{\omega} \frac{1}{|\omega| \eta_2(\omega)} \cdot \frac{1}{(1 + |\bar{\omega}|)^4} \quad (B.6)$$

$$B_{a-7} = -N_i \bar{\phi}_1^4 T \sum_{\omega} \frac{1}{(1 + |\bar{\omega}|)^4} \quad (B.7)$$

$$B_{a-8} = -4N_i \bar{\phi}_1 T \sum_{\omega} \frac{1}{[|\omega| \eta_2(\omega)]^3} \cdot \frac{1}{(1 + |\bar{\omega}|)^3} \quad (B.8)$$

$$B_{a-9} = 4N_i \bar{\phi}_1 T \sum_{\omega} \frac{1}{[|\omega| \eta_2(\omega)]^3} \cdot \frac{1}{(1 + |\bar{\omega}|)^4} \quad (B.9)$$

$$B_{a-10} = -4N_i \bar{\phi}_1^2 T \sum_{\omega} \frac{1}{|\omega| |\eta_2(\omega)|^2} \cdot \frac{1}{(1+|\bar{\omega}|)^4} \quad (B.10)$$

Summing up the contributions from the diagram (a-1) to (a-4) (we denote the total contribution as B_1), we immediately have as the leading term contribution

$$B_1 = -\frac{\pi N_i \rho}{2} T \sum_{\omega} \frac{|\omega| (1 + \frac{N_i}{4T_K \rho})}{[|\omega| \eta_2(\omega)]^4} + \dots \quad (B.11)$$

While summing up the contributions from the diagram (a-8) to (a-10) (we denote the total contribution as B_2), we have

$$B_2 = -4N_i \bar{\phi}_1 [T \sum_{\omega} \frac{|\bar{\omega}|}{|\omega| [|\omega| \eta_2(\omega)]^3} \cdot \frac{1}{(1+|\bar{\omega}|)^4} + \bar{\phi}_1^T \sum_{\omega} \frac{1}{|\omega| [|\omega| \eta_2(\omega)]^2} \cdot \frac{1}{(1+|\bar{\omega}|)^4}] \quad (B.12)$$

From these calculations, one finds that the second term of B_1 gives the order of $\frac{N_i}{T_K T^2}$ and that the first and second terms of B_2 give no more than the order of $\frac{N_i}{T_K T^2} T \bar{\phi}_1$ and $\frac{N_i}{T_K T^2} T T_K \bar{\phi}_1^2$, respectively. Therefore B_2 may be omitted as far as the condition $T \ll T_K$ is satisfied. The contributions from the diagram (a-5) to (a-6) may also be omitted for the same reason as B_2 . Furthermore, the diagram (a-7), B_{a-7} can be neglected, because this gives no more than the order of $\frac{N_i}{T_K T^2} (\frac{T}{T_K})^2 \phi_1^4$.

type (b)

As regards the non Hartree-Fock type contributions, we give order-of-magnitude discussions. The contribution from the diagram (b-1), B_{b-1} gives the order of $\frac{N_i}{T_K T^2} (\frac{T}{T_K})^2 \phi_1$. The contribution from the

diagram (b-2), B_{b-2} gives the order of $\frac{N_i}{T_K T^2} \left(\frac{T}{T_K}\right)^3 \phi_1^2$. We find that the (b)-type diagrams with more than two crossing lines of the effective interaction between d-electrons are no more than the same order as ones without crossing lines. Therefore all of the (b)-type contributions may also be omitted for reasons of the higher-order contributions to $B(T)$, though the diagrams with more than two crossing lines can never be calculated analytically.

References

- 1) T. Matsuura and Y. Nagaoka, Solid State Comm. 18 (1976), 1583.
T. Matsuura, S. Ichinose and Y. Nagaoka, Prog. Theor. Phys. 57, No.3, (1977).
- 2) E. Müller-Hartmann and J. Zittartz, Phys. Rev. Letters 26 (1971), 428.
E. Müller-Hartmann and J. Zittartz, Solid State Comm. 11 (1972), 401.
E. Müller-Hartmann and J. Zittartz, Z. Physik 256 (1972), 366.
- 3) K. Maki, J. Low Temp. Phys. 6 (1972), 505.
- 4) H. Shiba, Solid State Comm. 11 (1972), 1735:
Prog. Theor. Phys. 50 (1973), 50.
- 5) A.A. Abrikosov and L.P. Gor'kov, J. Exptl. Theoret. Phys. (U.S.S.R.) 39 (1960), 1781 [Sov. Phys. JETP, 12 (1961), 1243.]
- 6) P. Nozieres, J. Low Temp. Phys. 17 (1974), 31.
- 7) K.G. Wilson, Rev. Mod. Phys. 47 (1975), 773.
- 8) H. Shiba, Prog. Theor. Phys. 40 (1968), 435.
- 9) K. Yamada, Prog. Theor. Phys. 53 (1975), 970.
K. Yosida and K. Yamada, Prog. Theor. Phys. 53 (1975), 1286.
- 10) K. Takanaka and T. Nagashima, Prog. Theor. Phys. 38 (1967), 291.
- 11) C.A. Luengo, J.M. Cotignola and J.G. Sereni, Solid State Comm. 10 (1972), 459.
- 12) A.A. Abrikosov, Physics 2, (1965), 5.
- 13) P.W. Anderson, G. Yuval and D.R. Hamann, Phys. Rev. B1 (1970), 4464.
P.W. Anderson and G. Yuval, "Magnetism V", edited by H. Suhl, p.217, Academic Press (1973).
- 14) T. Matsuura, to be published in Prog. Theor. Phys.

Figure Captions

- Fig. 1 Diagrams of the contributions to $B(T)$ in the magnetic region. The solid line shows the propagator of the s-electron, while the impurity scattering by one and the same impurity atom is shown with dotted lines. The crosses represent the spin-flip part of the t-matrix $(\vec{\sigma} \cdot \vec{S})\tau(\omega)$, while the spin-non flip part $t(\omega)$ is attached to the squares. The vertex correction $\gamma(\omega)$ is attached to the four corners of the each diagram.
- Fig. 2 Diagrams of the contributions to $B(T)$ in the nonmagnetic region. (a) is the Hartree-Fock type contribution, and (b) is the non-Hartree-Fock type one. The single solid and double lines represent the propagators of s and d electrons. The wavy lines represent the repulsive interaction between d-electrons and are given as $\Gamma_d = \pi^2 \Gamma^2 / 4T_K$. $\gamma(\omega)$ is attached to the four corners of the each diagram, as before. Notice that symbols which display the impurity scattering by one and the same impurity atom are omitted for the reason of avoiding the complication of graphs.
- Fig. 3 The frequency dependence of the parameter $\chi(\omega)$ given in Eq. (3.14).
- Fig. 4 The specific heat jump at T_c as a function of T_c/T_{co} . Numbers attached to each curve denote the ratio T_K/T_{co} .
- Fig. 5 The initial slope of the specific heat jump as a function of T_K/T_{co} .

Fig. 1

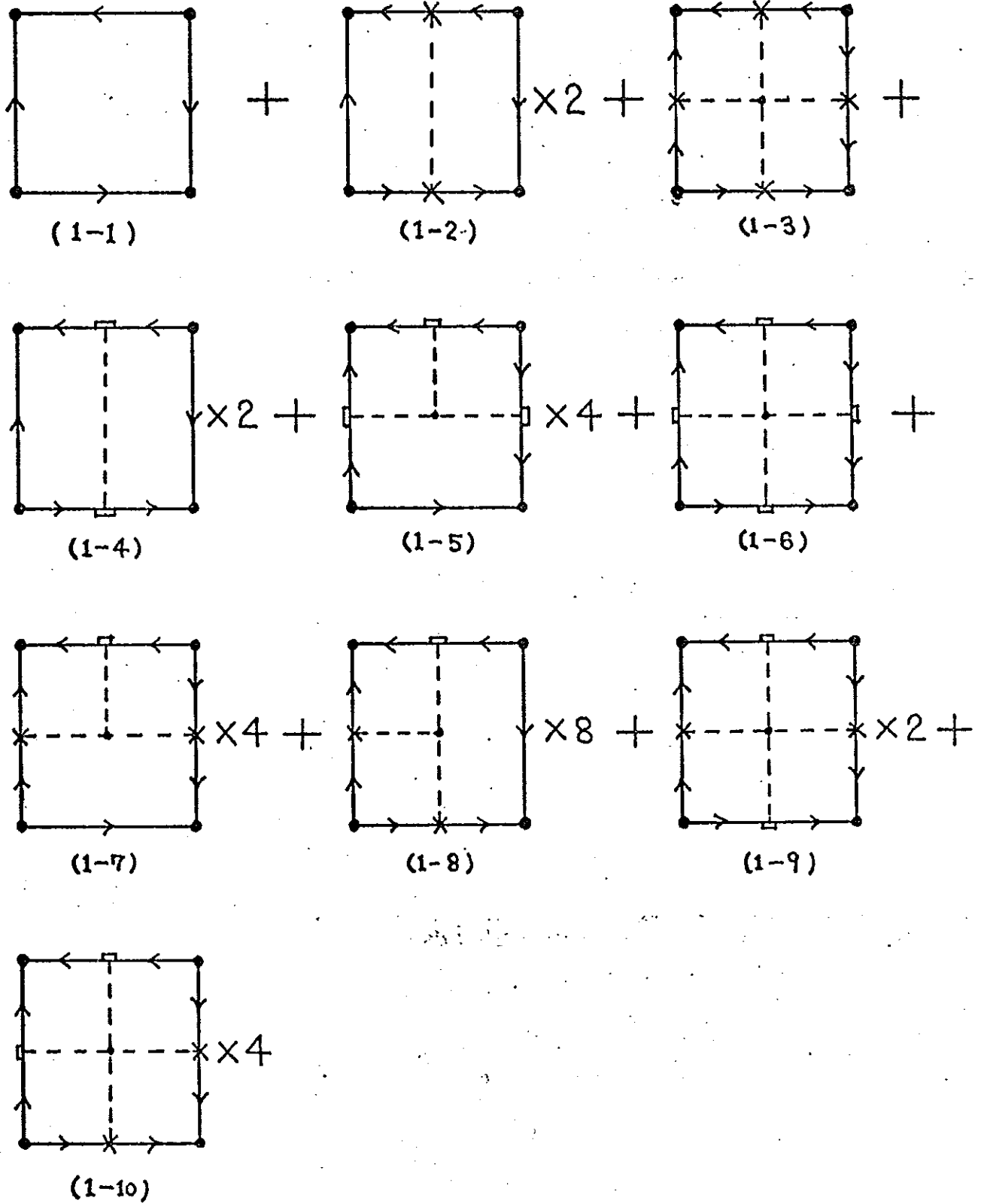
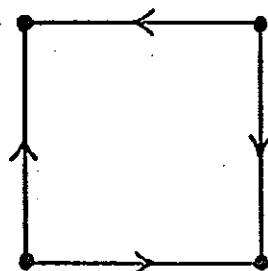
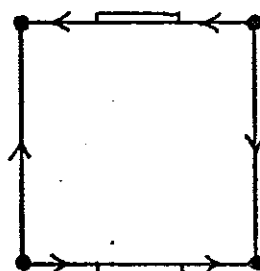


Fig. 2 (a)



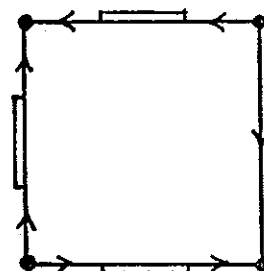
(a-1)

+



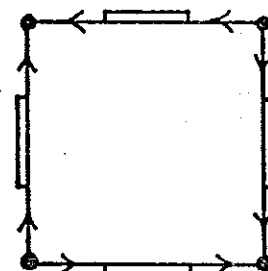
(a-2)

$\times 2$ +



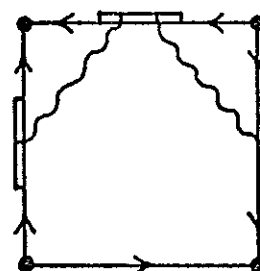
(a-3)

$\times 4$ +



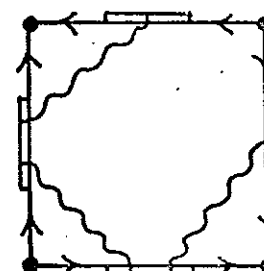
(a-4)

+



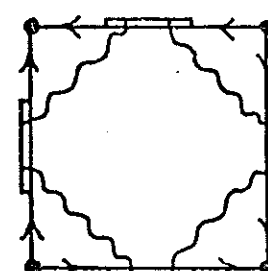
(a-5)

$\times 4$ +



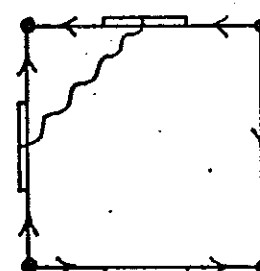
(a-6)

$\times 4$ +



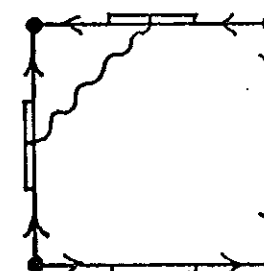
(a-7)

+



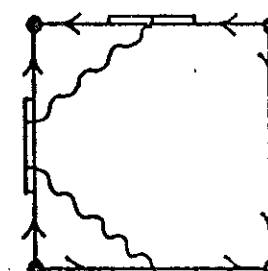
(a-8)

$\times 8$ +



(a-9)

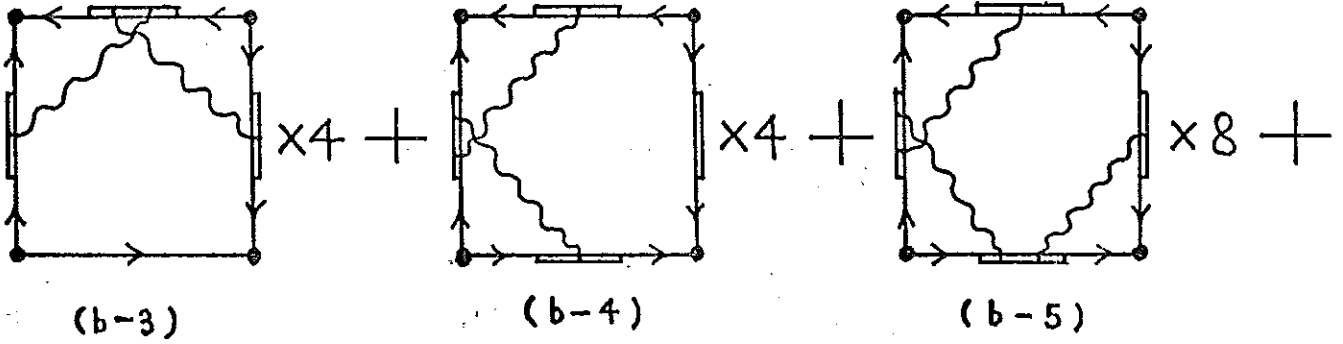
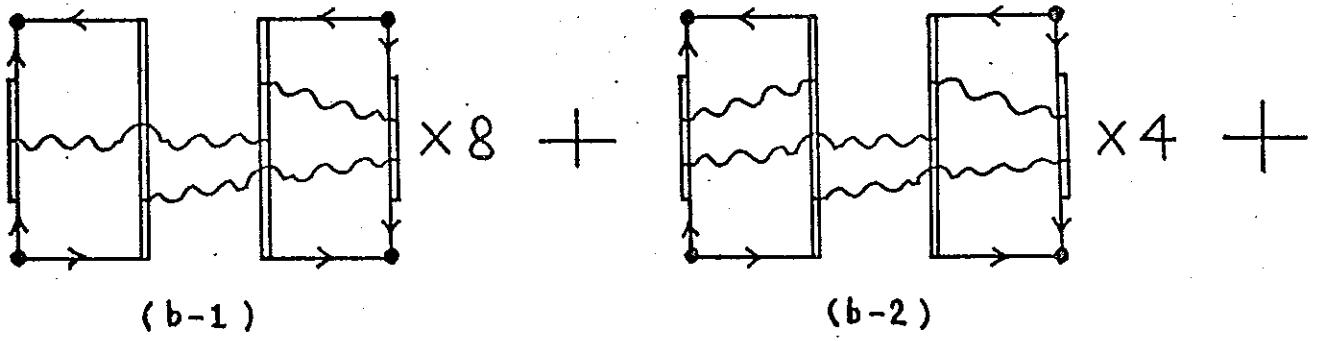
$\times 4$ +



(a-10)

$\times 4$ +

Fig. 2 (b)



+

Fig. 3

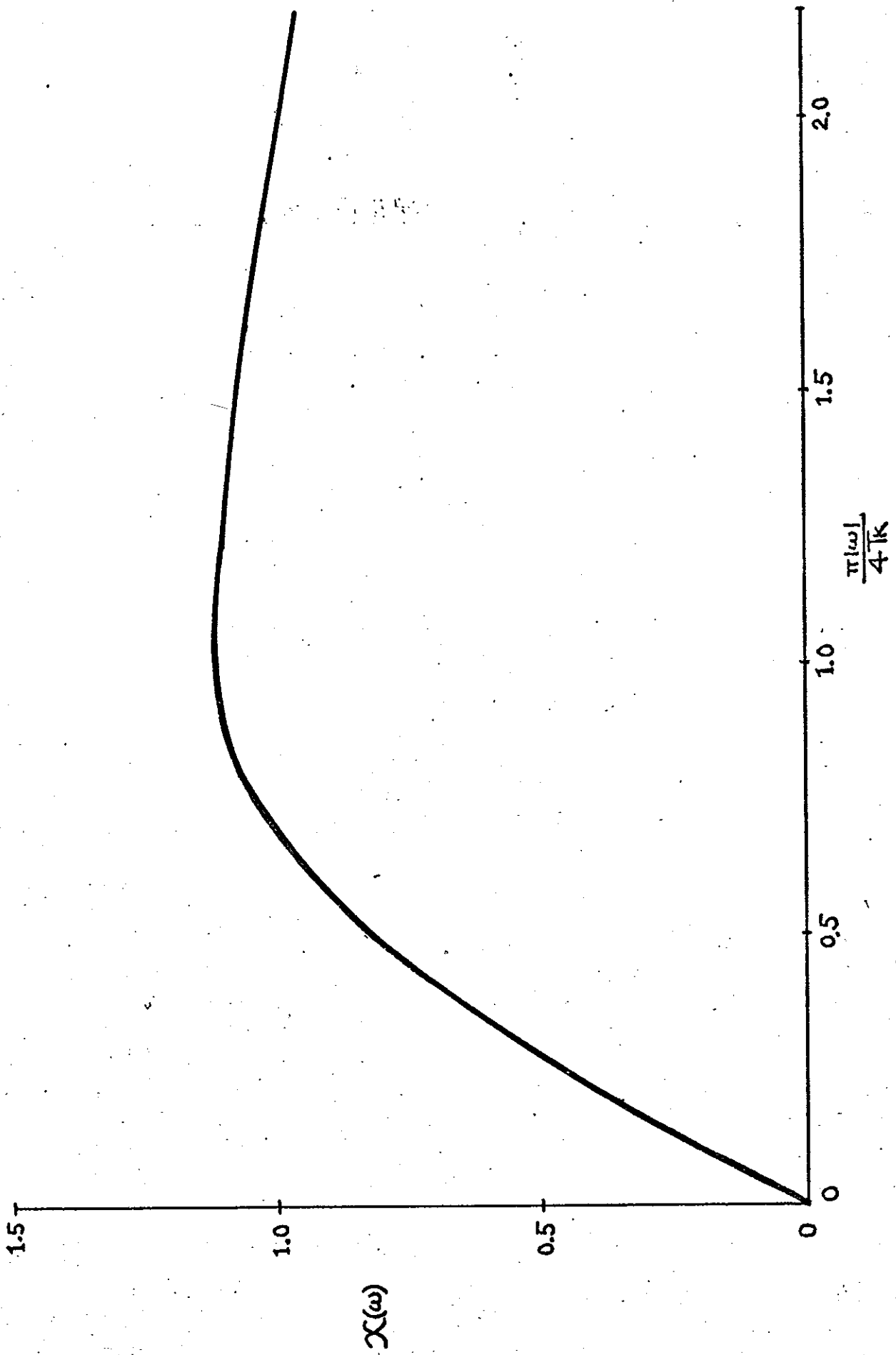


Fig. 4

| | |
|--------------------|---|
| T_k/T_{c0} | |
| 1×10^{-5} | 1 |
| 1×10^{-3} | 2 |
| 1×10^{-1} | 3 |
| 1 | 4 |
| 3 | 5 |
| 10 | 6 |
| 100 | 7 |

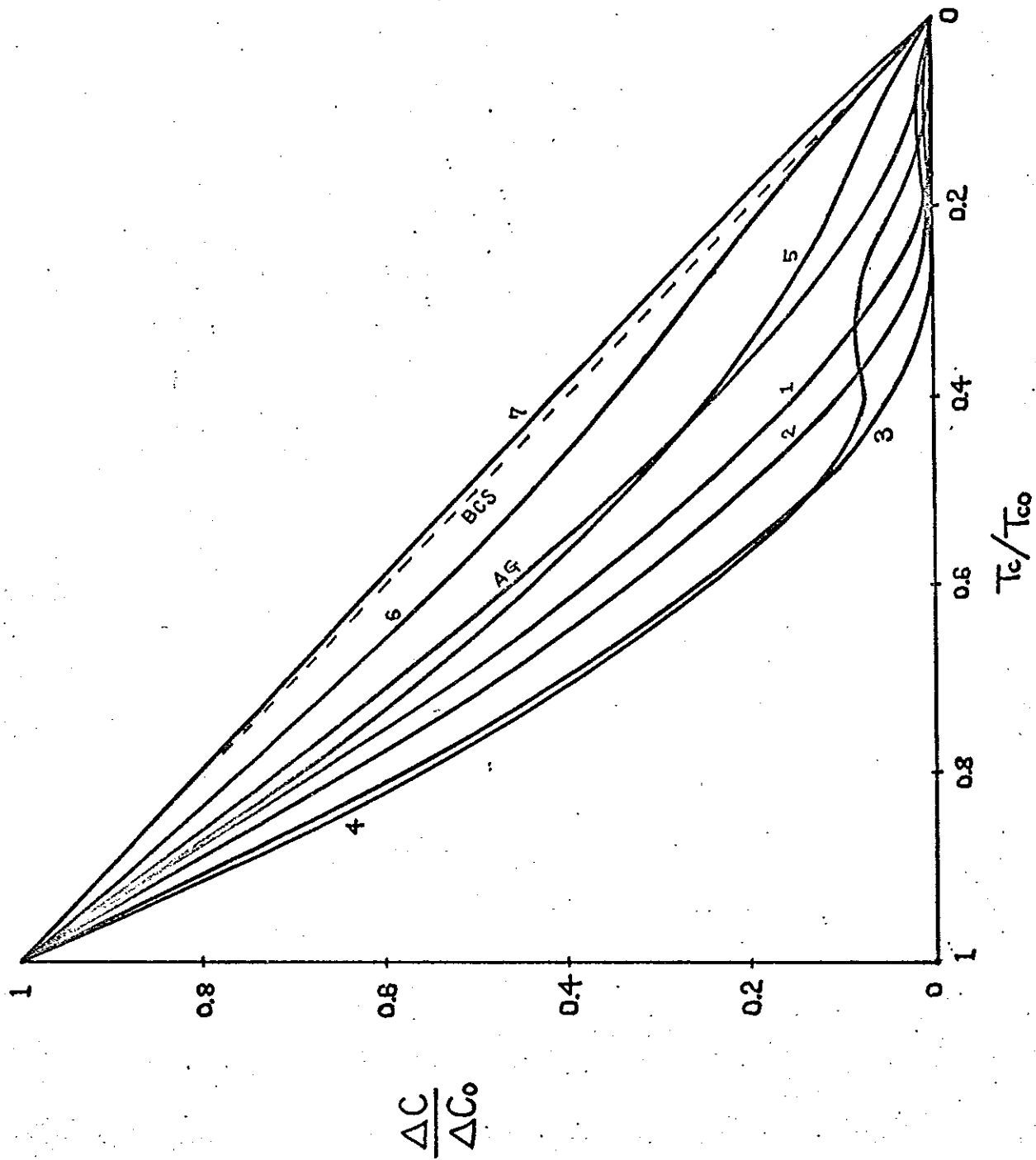


Fig. 5 $S = \frac{1}{2}$

